BILINGUAL PUBLISHING GROUP
Pioneer of Global Academics Since 1984

Journal of Mechanical Materials and Mechanics Research
https://journals.bilpubgroup.com/index.php/jmmmr

ARTICLE

Numerical Solution for Thermal Elastohydrodynamic Lubrication of Line Contact with Couple Stress Fluid as Lubricant

Vishwanath B. Awati[1*], Mahesh Kumar N[1], N.M. Bujurke[2]

[1] *Department of Mathematics, Rani Channamma University, Belagavi, 591156, India*
[2] *Department of Mathematics, Karnatak University, Dharwad, 580003, India*

ABSTRACT

In this paper, the detailed analysis of the influence of thermal and non-Newtonian aspects of lubricant (couple stress fluid) on EHL line contact as a function of slide-roll ratio is presented. The novel low complexity FAS (full approximation scheme), of the multigrid scheme, with Jacobi dipole and Gauss Seidel relaxation is used for the solution of coupled equations viz. modified Reynolds equation, film thickness equation and energy equation satisfying appropriate boundary conditions. The analysis reveals the combined influence of non-Newtonian, thermal and slide-roll ratio (of bearing moving with different speeds) on pressure, film thickness and pressure spike covering a wide range of physical parameters of interest. Results show that pressure spike is strongly influenced by thermal, slide-roll ratio and non-Newtonian character of lubricant with negligible effect on the overall pressure distribution. Also, the minimum film thickness is slightly altered and it increases with the increase in the couple stress parameter. These findings confirm the importance of non-Newtonian and thermal effects in the study of EHL.

Keywords: Thermal EHL; Slide-roll ratio; Couple stress fluid; Multigrid FAS; Non-Newtonian

1. Introduction

Elastohydrodynamic lubrication (EHL) is primarily concerned with the lubrication of contacting surfaces (machine elements) where the high pressure generated, due to high load and speed, in the cavity results in the deformation of (contacting) surfaces. This in turn causes changes in pressure developed and in this process the basic properties of the lubricant are affected. The viscosity and density of the

*CORRESPONDING AUTHOR:
Vishwanath B. Awati, Department of Mathematics, Rani Channamma University, Belagavi, 591156, India; Email: awati_vb@yahoo.com

ARTICLE INFO
Received: 10 January 2023 | Revised: 30 January 2023 | Accepted: 1 March 2023 | Published Online: 15 March 2023
DOI: https://doi.org/10.30564/jmmmr.v6i1.5396

CITATION
Awati, V.B., Mahesh, K.N., Bujurke, N.M., 2023. Numerical Solution for Thermal Elastohydrodynamic Lubrication of Line Contact with Couple Stress Fluid as Lubricant. Journal of Mechanical Materials and Mechanics Research. 6(1): 22-35. DOI: https://doi.org/10.30564/jmmmr.v6i1.5396

lubricant are functions of pressure and temperature. Due to the high speed of contacting surfaces thermal effects will have a considerable influence on EHL lubrication. In the contact region the pressure becomes very large (0.5 GPs to 3 GPs). With large speed film thicknesses reduces to some micrometers and as such wide range of scales is involved in EHL. Dowson and Higginson [1] and periodical review on EHL viz Hamrock and Tripp [2], Dowson and Ehrel [3], Schlijper et al. [4], Spikes [5], Lugt and Morales-Espejel [6] and others provide comprehensive developments (both theoretical schemes and experimental findings) in EHL line as well as point contact problems. Dissertations of Venner [7] and Goodyer [8] and others present many salient features of EHL problems.

The numerical investigation of EHL line contact problems, with Barus viscosity-pressure relation by Petrusevich [9] predicts a second pressure spike near the exit, which is one of the important features of EHL. In the inlet region (considering lubricant flow from left to right) the lubricant is fully flooded, the center (Hertzian contact) is a high-pressure region and again at the exit (out flow) the pressure is zero (cavitation region). Finite difference and finite element methods are commonly used in the EHL investigation. The studies pertaining to a wide range of parameters involved (especially those of high load cases) with algorithms of lower complexity could overcome the limitations of conventional numerical schemes. Okamura [10] presents the numerical solution of isothermal EHL by using the Newton-Raphson method. Lubrecht et al. [11] used a multigrid method introduced by Brandt [12], to solve EHL problems. Later, Brandt and Lubrecht [13] developed MLMI method for the fast evaluation of elastic deformation integral. Full approximation schemes (with Jacobi dipole relaxation) and others played a significant role in easing numerical studies of EHL problems by Venner [14], further details and finer aspects can be found in Venner [7]. Recently, Bujurke et al. [15] used the wavelet preconditioned Newton-GMRES method for the solution of EHL line contact analysis and demonstrate the efficiency of the solver in overcoming the limitations of conventional numerical schemes.

For the pressure and effective modeling of EHL, especially in predicting minimum film thickness, in knowing the spread and height aspects of Petrusevich pressure spike, resulting surface stresses and other aspects of bearing lubrication, it is essential to incorporate the influence of rheology (non-Newtonian nature) of lubricants and thermal effects. Bell [16] was the earliest investigator to predict the importance of lubricant rheology on film thickness using Grubin type method. Houpert and Hamrock [17], Conry et al. [18] solve isothermal EHL equation with Ree-Eyring type lubricant using Newton-Raphson method and cover a wide range of parameters of interest. Jacobson and Hamrock [19] use simplified limiting shear stress model lubricant and find a reduction in film thickness by solving the modified Reynolds equation and film thickness equation simultaneously. Zhu and Neng [20] present theoretical and experimental work on EHL with grease as a lubricant. Bujurke et al. [21] use Jacobian free Netwon-GMRES solver for the solution of EHL line contact problem with grease as a lubricant and present spread and height of Petrusevich pressure spike as a function of a parameter characterizing grease lubricant. Wang et al. [22] use the power law rheological model for the line contact EHL studies under pure rolling and find the location of the cavitation point as a function of the power law exponent. Chippa and Sarangi [23] consider the couple stress fluid model in finite line contact EHL problem and observe that, the increase in film thickness is due to an increase in the couple stress parameter. Das [24] and Saini et al. [25] also use a couple of stress fluid models in their EHL line contact analysis using the conventional finite difference method. Kantli et al. [26] and Shettar et al. [27] use a couple of stress fluid models in their detailed investigation of the second pressure spike and use Jacobian-free Newton-GMRES and Newton-MG schemes respectively. It is of interest to find the entry of bio-based lubricants in EHL[28] which are later also used by Awati et al. [29], Awati and Shankar [30] to find its novel features in tribology. Sternicht et al. [31] were one of the earliest investigators to incorporate thermal effects in EHL

rolling/sliding line contact problem. Later by assuming mean viscosity across the fluid film region, Cheng and Sternicht [32] and Dowson and Whitaker [33] investigate thermal EHL line contact problems for finding minimum film thickness. Murch and Wilson [34], Ghosh and Hamrock [35] attempt in analyzing thermal effects on EHL, which are accurate for moderate parameters (weight and speed). Sadeghi and Sui [36] solve thermal EHL rolling/sliding line contact using a system approach, developed earlier by Houpert and Hamrock [37] and derived accurate film thickness formula. Yang and Wen [38], Wolff et al. [39] analyzed the lubrication problem based on thermal EHL rolling/sliding line contact model and obtained the tapered wedge shape of oil film under high rolling speed and slip conditions. Wolff and Kubo [40] presented the applications of Newton-Raphson method for the solution of thermal EHL line contacts. Hsiao and Hamrock [41], Yang et al. [42] use the combined influence of non-Newtonian and thermal effects on film thickness and surface stresses in EHL line contact problems. Other important studies on this aspect are due to Salahizadeh and Saka [43], over rolling aspects, and recently more effective/detail analysis by Liu et al. [44]. In most of the EHL papers, the solutions of EHL-line contact problems were solved by using Newton-Raphson method. The demerits of Newton-Raphson method are that, the computational complexity of the method is of order $O(n^3)$, n is the number of calculation points in the calculation domain. The elastic deformations term is the Jacobian matrix which is a $n \times n$ matrix and obtaining its inverse requires $O(n^3)$ operations. Also, for high load and high speed the Jacobian becomes singular for a finer grid in employing the Newton-Raphson method. This difficulty can be overcome by using much lower complexity schemes for the solution. In this respect the computation complexity of the FAS method is of order $O(nlogn)$ which is a more efficient method compared to Newton-Raphson.

Multigrid FAS method [45]

The nonlinear system of algebraic equations can be written as $L^h(u^h) = f^h$, where L^h is the nonlinear operator, u is the exact solution, f is the right hand side and h is the mesh size of a uniform finer grid. Let v be an approximation to the exact solution then $e^h = u^h - v^h$ denotes the error and $r^h = f^h - L^h(v^h)$ represents the residue. In FAS, instead of solving the error in the next coarser grid by restricting the residue, the system of nonlinear equations is solved with a modified right-hand side, i.e. $f^{2h} = I_h^{2h} r^h + L^{2h}(I_h^{2h} v^h)$. Continuing this process till the coarsest level H is reached and error is computed as $e^H = u^H - v^H$. This error is added to the solution obtained in the next fine grid by interpolation and relaxation to get a new solution. Error is computed and this process is repeated until the finest level is reached.

The schematic representation of two grid FAS cycle is as follows:

1) Relax $L^h(u^h) = f^h$ with a few relaxations on a fine grid with an initial value u_0^h to get v^h.

2) Compute residue $r^h = f^h - L^h(v^h)$ and restrict residue r^h and v^h to a coarser grid.

3) Compute modified RHS as $f^{2h} = I_h^{2h} r^h + L^{2h}(I_h^{2h} v^h)$ and relax $L^{2h}(u^{2h}) = f^{2h}$ with the initial guess $v^{2h} = I_h^{2h} v^{2h}$.

4) Calculate error $e^{2h} = u^{2h} - v^{2h}$ and interpolate to finer grids and add to v^h.

5) Again relax $L^h(u^h) = f^h$ with v^h to get an approximate solution.

2. Mathematical formulation

Consider two infinitely long cylinders that are rolling at speeds u_1 and u_2, separated by a lubricant (here couple stress fluid) and supporting a load W per/unit axial length. The elastic cylinders are of radius R_1 and R_2 with elastic moduli E_1, E_2 and of Poisson's ratio v_1 and v_2 respectively. As rollers support high loads they experience elastic deformation in the central or Hertz contact region. With usual assumptions [1] the lubricant film thickness in dimensionless form is:

$$H(\mathrm{X}) = \mathrm{H}_0 + \frac{X^2}{2} + \overline{V} \tag{1}$$

where $H_0 = \frac{h_0 R}{b^2}$, $\frac{1}{R} = \frac{1}{R_1} + \frac{1}{R_2}$, b is the half width of

Hertz contact zone, $H=\frac{hR}{b^2}$, h is the film thickness and h_0 is offset film thickness.

$$\overline{V}=\frac{-1}{2\pi}\int_{X_{in}}^{X_{out}}P(X)Log(\mathrm{X-S})^2\,\mathrm{dS} \tag{2}$$

P is dimensionless pressure buildup in the lubricant cavity, X_{in}, X_{out} are inlet and outlet boundary co-ordinates (location) and $X=\frac{x}{b}$.

The dimensionless steady-state Reynolds equation for compressible couple stress fluid as a lubricant is given by Saini et al. [25].

$$\frac{\partial}{\partial X}\left(\frac{\overline{\rho}H^3}{\overline{\eta}\ \xi}\frac{dP}{dX}\right)-K\frac{d}{dX}(\overline{\rho}H)=0 \tag{3}$$

where $\xi=\left[1-\frac{12}{\Omega^2}+\frac{12}{\Omega^3}\tanh\left(\frac{\Omega}{2}\right)\right]^{-1}$, $L_m=\frac{\lambda_a}{R}$, $\Omega=\frac{8WH}{\pi L_m}$, $K=\frac{3U\pi^2}{4W^2}$, L_m is a dimensionless couple stress parameter and λ_a is the molecular length of additive.

The dimensionless load balance equation is:

$$\int_{X_{in}}^{X_{out}}P(X)dX=\frac{\pi}{2}. \tag{4}$$

The Roelands [46] relation, in dimensionless form, connecting viscosity-pressure-temperature is:

$$\overline{\eta}=\exp\left[\left\{\ln(\eta_0)+9.67\right\}\left[-1+\left(1+5.1\times10^{-9}P_HP\right)^{\overline{z}}\right]+\gamma T_0(1-T)\right]. \tag{5}$$

where η_0 is the absolute viscosity, $P_H=\frac{p_h}{p_0}$ is ambient pressure and $\overline{z}$ is a constant characteristic of the liquid (pressure-viscosity index). The modified form of Dowson-Higginson [1] relation about density-pressure-temperature in dimensionless form is:

$$\overline{\rho}=\left[1+\frac{0.6\times10^{-9}P_HP}{1+1.7\times10^{-9}P_HP}\right]\left\{1-\beta T_0(T-1)\right\}. \tag{6}$$

The boundary conditions for the pressure distribution are:

$$P(X_{in})=0;\ \text{and}\ P(X_{out})=\frac{dP}{dX}=0 \qquad at\ \ \mathrm{X}=\mathrm{X}_{out}. \tag{7}$$

Energy equation

Assume the lubricant properties such as thermal conductivity, specific heat and thermal expansivity to be constants with respect to pressure and temperature than the energy equation in dimensionless form is [47]:

$$\frac{\partial^2T}{\partial\overline{Z}^2}=K_3\overline{\rho}H^2\left(\overline{U}\frac{\partial T}{\partial X}\right)-K_2H^2T\left(\overline{U}\frac{\partial P}{\partial X}\right)-K_1\frac{\overline{\eta}}{\phi}\overline{\tau}\left(\frac{\partial\overline{U}}{\partial\overline{Z}}\right) \tag{8}$$

where, $K_1=\frac{(E'RU)^2}{T_0\eta_0k}$, $K_2=\frac{\beta(E'R)^2U}{4\eta_0k}\left(\frac{8W}{\pi}\right)^2$, $K_3=\frac{c\rho_0E'R^2U}{\eta_0k}\left(\frac{8W}{\pi}\right)^{3/2}$ and $\varphi=\frac{\pi U\overline{\eta}}{8WH}$, $u=u_a+\frac{u_b-u_a}{h}z+\frac{1}{2\eta}\frac{\partial p}{\partial x}\left\{z^2-hz+2\lambda_a^2\left[1-\frac{\cosh(2z-h)/2\lambda_a^2}{\cosh(h/2\lambda_a)}\right]\right\}$, from Siani et al [25]. $\overline{\tau}=\frac{\tau}{E'}$ and τ is shear stress of the couple stress fluid and is given by $\tau=\eta\left(\frac{\partial u}{\partial z}-\lambda_a^2\frac{\partial^3u}{\partial z^3}\right)$.

The associated boundary conditions for the energy equation becomes:

$$T(X,0)=T_a;\ \ T(X,H)=T_b \tag{9}$$

where T_a and T_b are the lower and upper surface temperatures of bearing surfaces and are given by [37]:

$$T_a(X)=1+\frac{k_f(\eta_0)^{1/2}(\pi/8W)^{3/4}}{\sqrt{\pi\rho_1c_1k_1[E'U(1-s/2)]R}}\int_{X_i}^{X}\frac{1}{H}\left(\frac{\partial T}{\partial\overline{Z}}\right)_{\overline{Z}=0}\frac{dX'}{\sqrt{X-X'}} \tag{10}$$

$$T_b(X)=1+\frac{k_f(\eta_0)^{1/2}(\pi/8W)^{3/4}}{\sqrt{\pi\rho_2c_2k_2[E'U(1+s/2)]R}}\int_{X_i}^{X}\frac{1}{H}\left(\frac{\partial T}{\partial\overline{Z}}\right)_{\overline{Z}=1}\frac{dX'}{\sqrt{X-X'}} \tag{11}$$

The mean dimensionless temperature T_m is obtained as follows:

$$T_m=\int_0^1Td\overline{Z} \tag{12}$$

In fact, the surface temperatures T_a and T_b (mentioned above) are not known in advance. The heat generated in the lubricant is due to roller surfaces experiencing continuous heat flux from the lubricant film as it moves through the contact area. This temperature rise at the surface of rollers is equivalent to a stationary semi-infinite solid subjected to a moving heat source on its surface which is an elegant work-out problem in Carslaw and Jaeger [48] and this solution is the notation of our boundary conditions on T_a and T_b mentioned above.

3. Discretization of governing equations

The Equations (1)-(3) and (8) are discretized using second-order finite difference approximation with grid size (with a number of grid points N) $N=512$ in the spatial domain of computation i.e.

$[X_{in}, X_{out}]=[-4, 1.5]$ and X_c, the cavitation point to be determined during the solution process. The discretized form of the Reynolds equation and relevant boundary conditions are:

$$\frac{\varepsilon_{i-1/2}P_{i-1}-(\varepsilon_{i-1/2}+\varepsilon_{i+1/2})P_i+\varepsilon_{i+1/2}P_{i+1/2}}{\Delta X^2}=K\frac{\rho_i H_i-\rho_{i-1}H_{i-1}}{\Delta X} \quad (13)$$

where, $\Delta X = X_i - X_{i-1}$, $\varepsilon_i = \frac{\overline{\rho_i} H_i^3}{\eta_i \xi_i}$ and $\varepsilon_{i\pm\frac{1}{2}} = \frac{\varepsilon_i \pm \varepsilon_{i\pm1}}{2}$,

$$P(X_{in})=0 \text{ and } \frac{P(X_{out})-P(X_{out-1})}{\Delta X}=0. \quad (14)$$

The film thickness equation in discretized form as:

$$H_i = H_0 + \frac{X_i^2}{2} + \frac{1}{2\pi}\sum_{j=1}^{N} D_{i,j}P_j, \quad (15)$$

where, $D_{i,j} = -\left(i-j+\frac{1}{2}\right)\Delta X\left[\text{h}\left(\left|i-j+\frac{1}{2}\right|\Delta X\right)-1\right]+\left(i-j+\frac{1}{2}\right)\Delta X\right)-1\Big]+\left(i-j+\frac{1}{2}\right)\Delta X\left[\text{h}\left(\left|i-j-\frac{1}{2}\right|\Delta X\right)-1\right]$ for $i=0,1,2,...,N$, $j=0,1,2,...,n$. The force balance equation in discretized form as:

$$\Delta X\sum_{i=1}^{N}\left(\frac{P_i+P_{i-1}}{2}\right)-\frac{\pi}{2}=0 \quad (16)$$

The energy equation in discretized form as:

$$\frac{1}{(\Delta\overline{Z})^2}(T_{k-1}-2T_k+T_{k+1}) = K_3\overline{\rho_k}H_i^2\overline{U}_k\left(\frac{T_{i,k}-T_{i-1,k}}{\Delta X}\right) - K_2H_i^2\overline{U}T_k\frac{\partial P}{\partial X}-K_1\frac{\overline{\eta_k}}{\varphi}\overline{\tau}\left(\frac{\partial\overline{U}}{\partial\overline{Z}}\right) \quad (17)$$

The convergence criteria for pressure and temperature becomes:

$$\frac{\sum(P_i^{k+1}-P_i^k)}{\sum P_i^{k+1}}\le\varepsilon \text{ and } \frac{\sum(T_i^{k+1}-T_i^k)}{\sum T_i^{k+1}}\le\varepsilon,$$

where, $\varepsilon = 1E-4$ is error tolerance.

4. Numerical method

We use Multigrid Full Approximation Scheme (FAS) for the solution of a nonlinear system of algebraic equations i.e. Equations (13) to (16) with relations Equations (5) and (6). The geometry and material parameters used are the ones given in Saini et al. [25] which pertain to broad aspects of (EHL line contact) bearing in use. The relaxation process in FAS is followed as described by Venner [14]. The coefficient ε in Equation (13) varies several orders of magnitude over the computational domain. The inlet and outlet regions $\varepsilon >> 1$ (η and H^3 are large), whereas in contact regions $\varepsilon << 1$ (η and H^3 are relatively small). For $\varepsilon >> 1$, Gauss-Seidel relaxation and for $\varepsilon << 1$, Jacobi dipole relaxation is applied with an under-relaxation factor of 0.3~0.6; and 0.1~0.3 respectively.

The procedure of FAS for EHL problem requires pressure correction in every grid but H_0 in load balance is corrected only on the coarsest grid. Let us assume that an approximate solution $\tilde{P}_i$, $\tilde{H}_i$ is obtained from Equation (15). The Gauss-Seidel relaxation process is applied in obtaining new approximation $\overline{P}_i$ in the region of large ε/h^2 and is given by:

$$\overline{P}_i = \tilde{P}_i + \left(\frac{\partial L_i^h}{\partial P_i}\right)^{-1} r_i,$$

where, r_i is the residual of the discrete Reynolds equation at i,

$$r_i = -(\varepsilon_{i-1/2}\overline{P}_{i-1}-(\varepsilon_{i-1/2}+\varepsilon_{i+1/2})\tilde{P}_i+\varepsilon_{i+1/2}\tilde{P}_{i+1})/h^2 + (\tilde{\rho}_i\tilde{H}_i-\tilde{\rho}_{i-1}\tilde{H}_{i-1})/h,$$

And $\frac{\partial L_i^h}{\partial P_i}$ is obtained:

i.e. $$\frac{\partial L_i^h}{\partial P_i} \approx -(\varepsilon_{i-1/2}+\varepsilon_{i+1/2})/h^2 + \frac{1}{\pi}(\tilde{\rho}_i K_{i,i}^{hh} - \tilde{\rho}_{i-1}K_{i-1,i}^{hh})/h.$$

The Jacobi dipole relaxation process is applied in the region of small ε/h^2 and pressure is updated as $\overline{P}_i = \tilde{P}_i + \delta_i$ and $\overline{P}_{i-1} = \tilde{P}_{i-1} - \delta_i$. For the calculation δ_i we use:

$$\delta_i = \left(\frac{\partial L_i^h}{\partial P_i} - \frac{\partial L_i^h}{\partial P_{i-1}}\right)^{-1} r_i$$

where,

$$r_i = -(\varepsilon_{i-1/2}\tilde{P}_{i-1}-(\varepsilon_{i-1/2}+\varepsilon_{i+1/2})\tilde{P}_i+\varepsilon_{i+1/2}\tilde{P}_{i+1})/h^2 + (\tilde{\rho}_i\tilde{H}_i-\tilde{\rho}_{i-1}\tilde{H}_{i-1})/h$$

and,

$$\frac{\partial L_i^h}{\partial P_i} - \frac{\partial L_i^h}{\partial P_{i-1}} \approx -(2\varepsilon_{i-1/2}+\varepsilon_{i+1/2})/h^2 + \frac{2}{\pi}(\tilde{\rho}_i K_{i,i}^{hh} - \tilde{\rho}_{i-1}K_{i-1,i}^{hh})/h$$

The cavitation condition is obtained by replacing negative $\overline{P}_i$ values (in the calculation) with zero. There satisfy the load balance equation and H_0 is corrected as:

$$H_0 = H_0 - c\left(\frac{\pi}{2} - h\sum_{j=0}^{n-1}0.5\left(\overline{P}_j+\overline{P}_{j+1}\right)\right)$$

where c is a suitably chosen constant and $\overline{P}_j$ denotes the current approximation to P_j. The algorithm for the solution of the thermal EHL problem:

1) Solve the Reynolds equation by the FAS

method and apply MLMI method to solve elastic deformation with initial pressure and temperature.

2) Obtained pressure is used to solve energy equation by finite difference with the Gauss-Seidel iteration method.

3) The temperature in step 2) is again used to solve the Reynolds equation for pressure and thermal equation.

4) This process is repeated till convergence is achieved.

5. Result and discussion

Computations are performed using FAS with Jacobi dipole relaxation (Reynolds equation), MLMI (film thickness equation) and Gauss-Seidel (Temperature/heat equation) for various parameters and obtain pressure, film thickness and temperature distributions and details of a pressure spike. By using double precision arithmetic and confining to the stopping criterion of iteration as mentioned above. Profiles of P and H for various L_m with sliding ratio $s=0.5$ and $s=0.1$ are given in **Figure 1(a, b)** for the isothermal case and those in **Figure 2(a, b)** with thermal effect. Pressure in the inlet and Hertz contact region is not much affected by either couple stress or thermal effect. However, the pressure spike with the isothermal case and its influence is found that shift towards centre of the contact region with increasing L_m. These are shown with moderate load and speed for both $s=0.5$ and $s=0.1$. However, film thickness increases with increasing values of L_m for both isothermal and thermal cases. Profiles in **Figure 3(a, b)** are pressure and film thickness for varying load and moderate value of U and L_m with $s=0.5$ and $s=0.1$ respectively. Pressure spike has a noticeable sharp increase in height for $s=0.5$ compared with $s=0.1$. Not much change in other parts of P but there is a slight variation in minimum film thickness with increasing W. Profiles in **Figure 4(a, b)** are again for P and H with varying speed and fixed values of W and L_m for $s=0.5$ and $s=0.1$ respectively. Pressure spike has a marginal effect but film thickness decreases considerably for increasing values of U in both the cases of slide/rolling ratio. A similar observation is made with earlier theoretical models on EHL line contact by Wang and Zhang [47] using different rheological models and Saini et al. [25] a compressible couple stress fluid model. They employ Newton-Raphson method for their analysis of moderate load and moderate speed. The present solver overcomes these limitations and it enables to analyze of the problem by incorporating moderate to high load and high speed.

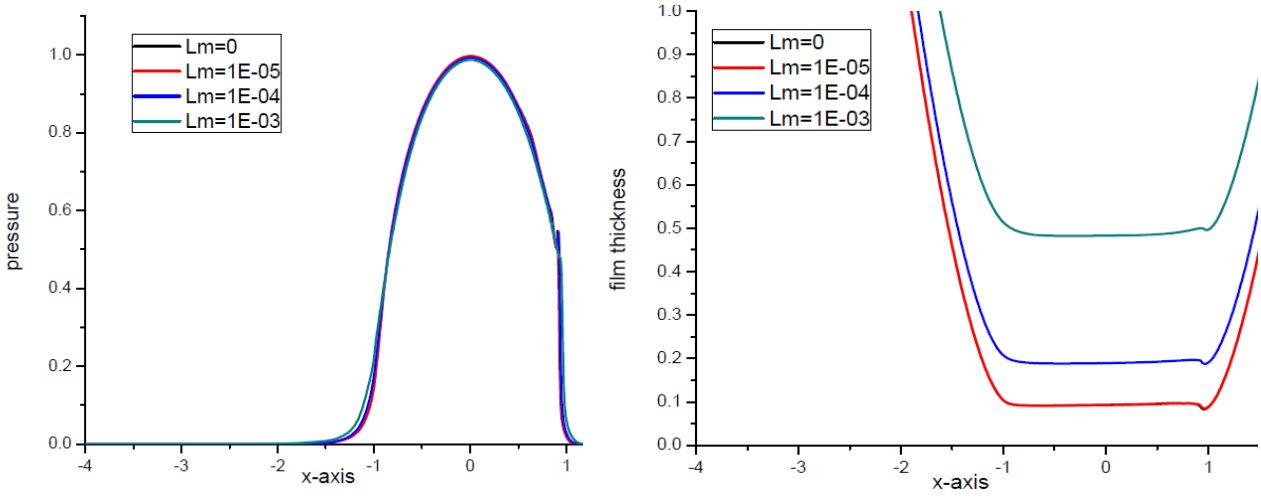

Figure 1a. Isothermal Pressure and film thickness profiles for varying L_m at U=2E-11, W=2E-04 and s=0.5.

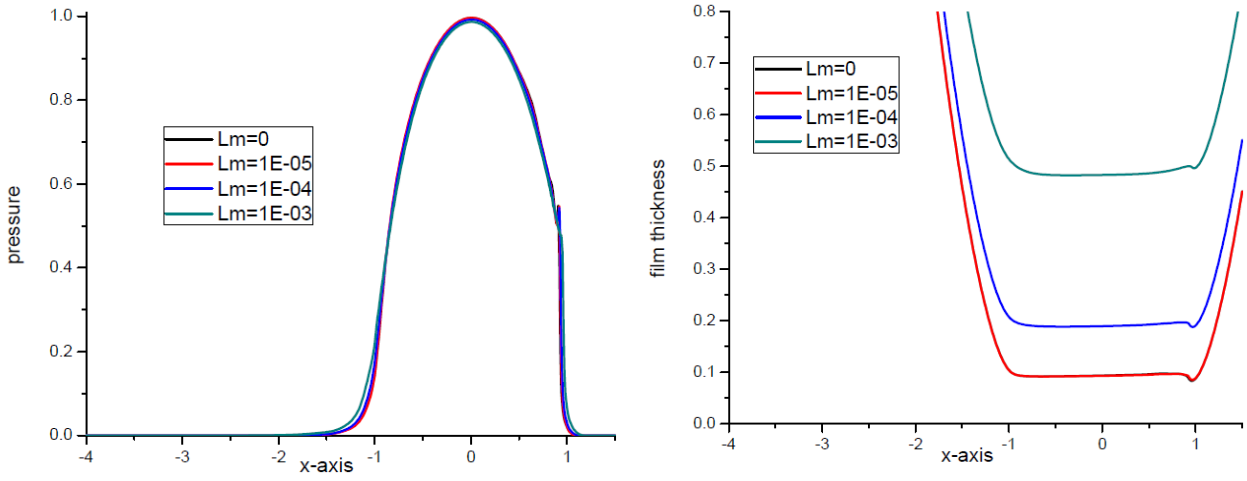

Figure 1b. Isothermal Pressure and film thickness profiles for varying L_m at U=2E-11, W=2E-04 and s=0.1.

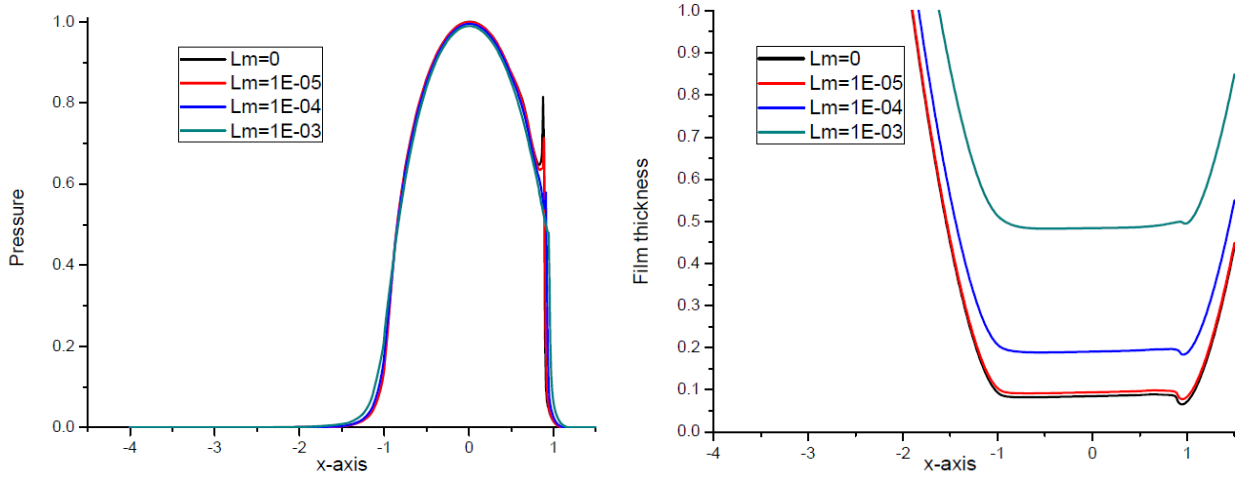

Figure 2a. Thermal pressure and film thickness profiles for varying L_m at U=2E-11,W=2E-04 and s=0.5.

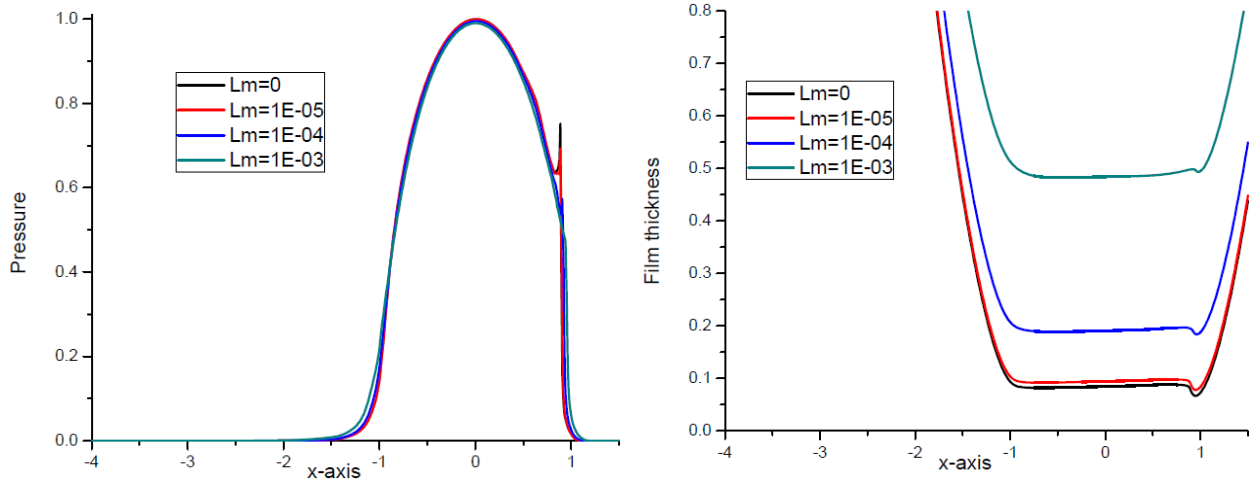

Figure 2b. Thermal pressure and film thickness profiles for varying L_m at U=2E-11,W=2E-04 and s=0.1.

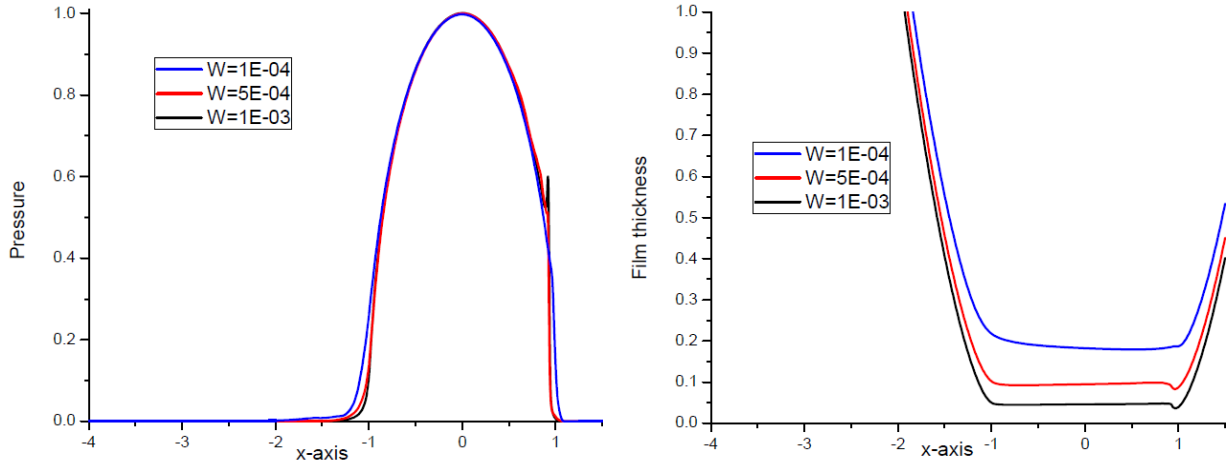

Figure 3a. Thermal pressure and film thickness profiles for varying W at U=2E-11, L_m =1E-04 and s=0.5.

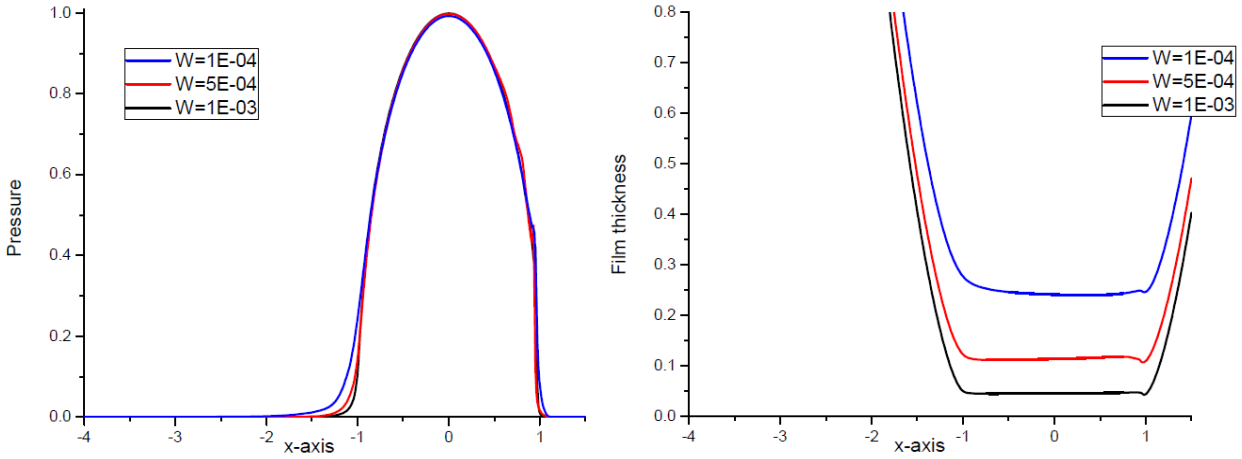

Figure 3b. Thermal pressure and film thickness profiles for varying W at U=2E-11, L_m =1E-04 and s=0.1.

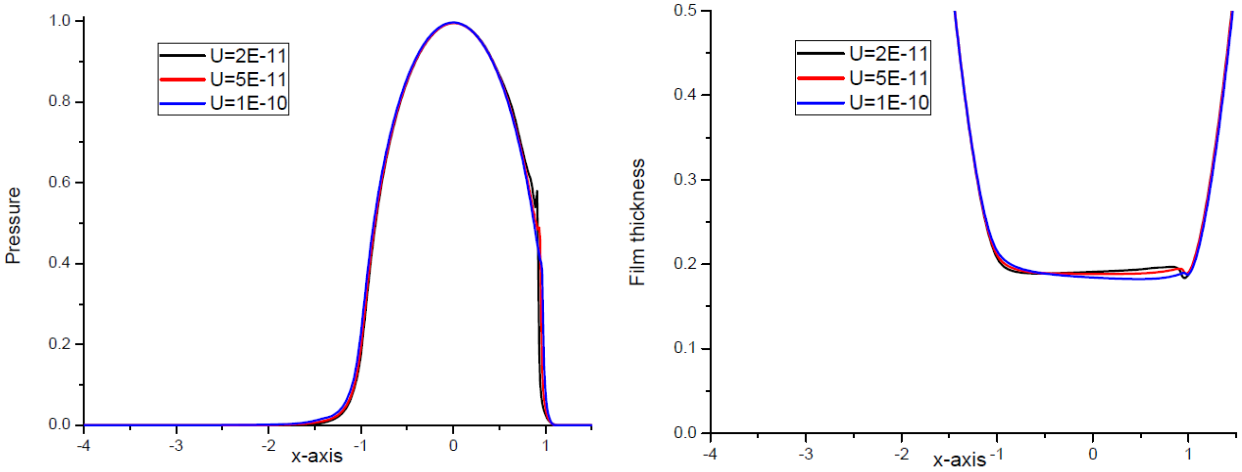

Figure 4a. Thermal pressure and film thickness profiles for varying U at W=2E-04, L_m =1E-04 and s=0.5.

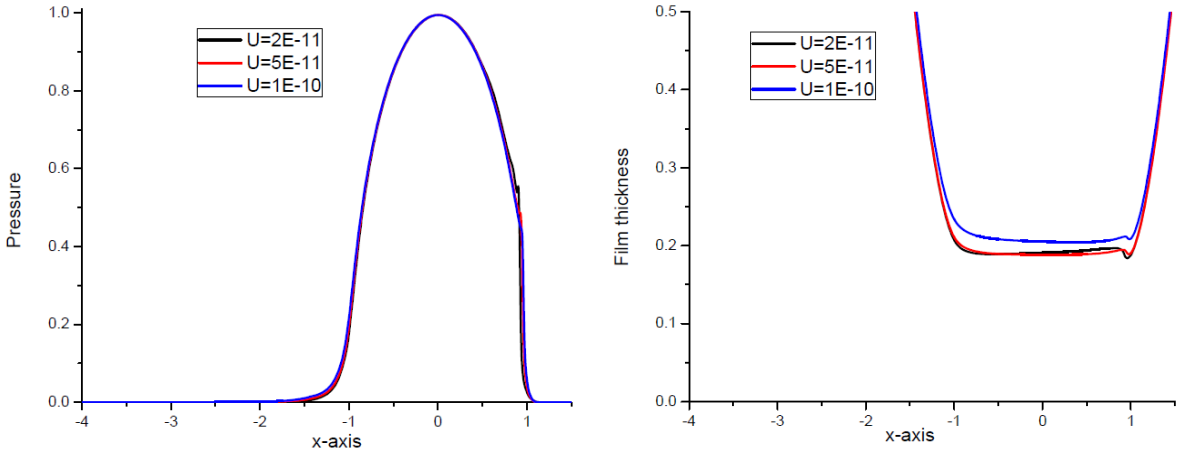

Figure 4b. Thermal pressure and film thickness profiles for varying U at W=2E-04, L_m =1E-04 and s=0.1.

The detailed analysis of pressure spikes is of much importance in bearing design. Earlier attempts on this topic are by Bisset and Glander [49], Venner and Napel [50] and Bujurke et al. [15] using different methods. Here, we present the pressure spike in an enlarged region to elucidate its details. In **Figure 5(a, b)** details of pressure spike (height, spread, location) with varying load and prescribed U and L_m are shown for $s=0.5$ and $s=0.1$ respectively. In Isothermal, case pressure spike decreases for increasing load but using thermal effect it has noticeable height and spread but shifts towards exit region. Much sharper profiles are observed for $s=0.5$ and compared with that of $s=0.1$. In **Figure 6(a, b)** profiles of pressure spikes are shown for varying L_m and fixed moderate W and U for both $s=0.5$ and $s=0.1$ respectively. Spike is spread in a larger region with greater height and it shifts slightly towards the center of the contact for increasing slide/rolling ratio with thermal effect. Spike structure analysis is a delicate issue but we just present our findings, which are qualitative. There is an increase in minimum film thickness with an increase in s compared with viscous lubricant. However, for both viscous and couple stress fluids there is a marginal decrease in minimum film thickness due to thermal effects. From profiles in **Figure 7(a, b)**, it is clear that, the pressure spike increases slightly whereas film thickness decreases considerably for the increase in slide-roll ratio. In **Figure 8** pressure spike in the enlarged region (of **Figure 7a**) is shown. Profiles in **Figure 8** show these assertions clearly.

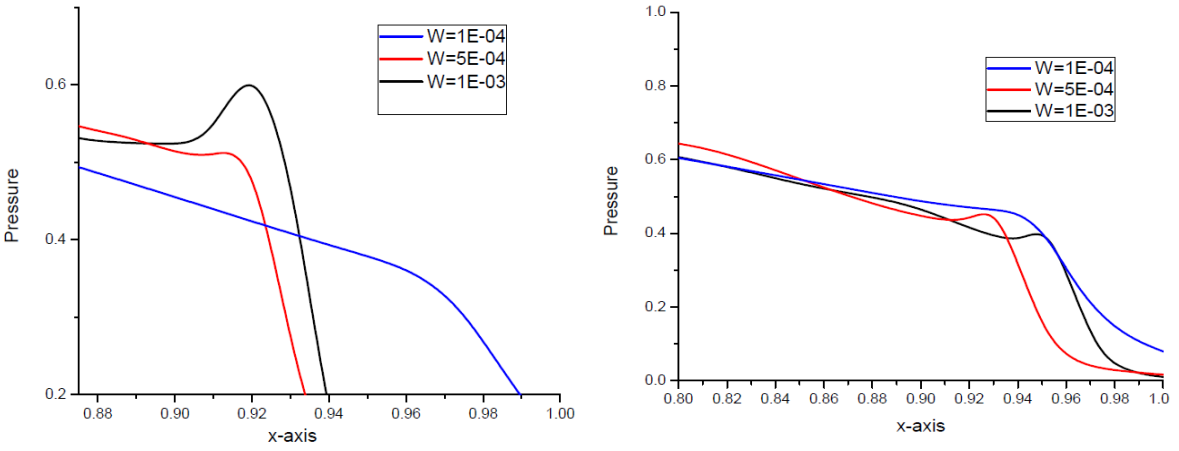

Figure 5. Thermal pressure spike for varying W at U=2E-11, L_m =1E-04, s=0.5(a) and s=0.1(b).

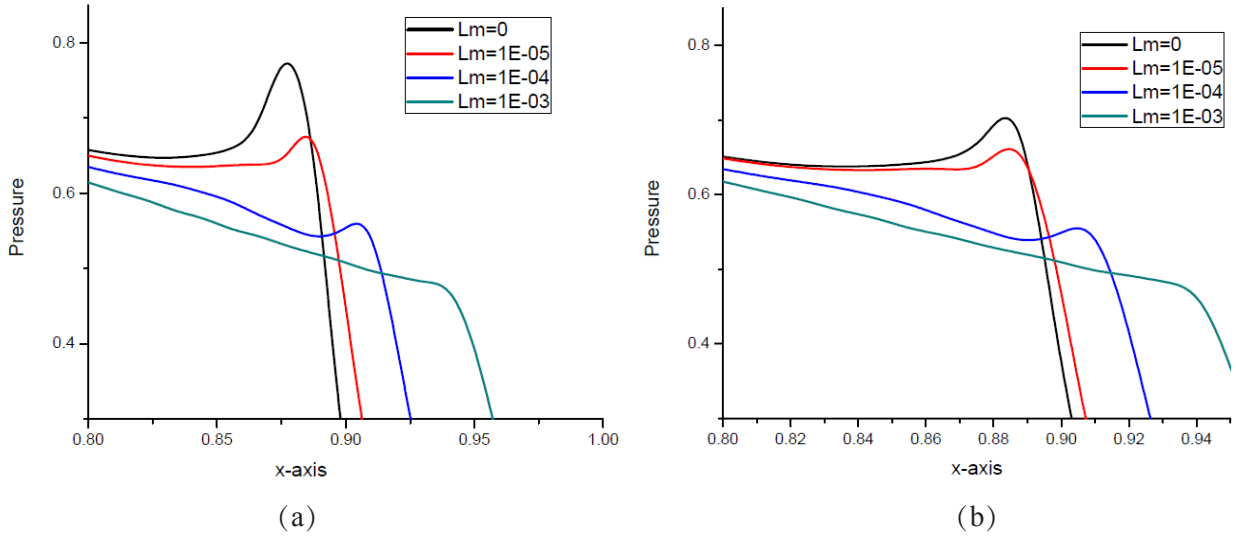

Figure 6. Thermal pressure spike for varying L_m at U=2E-11, W=2E-04, s=0.5(a) and s=0.1(b).

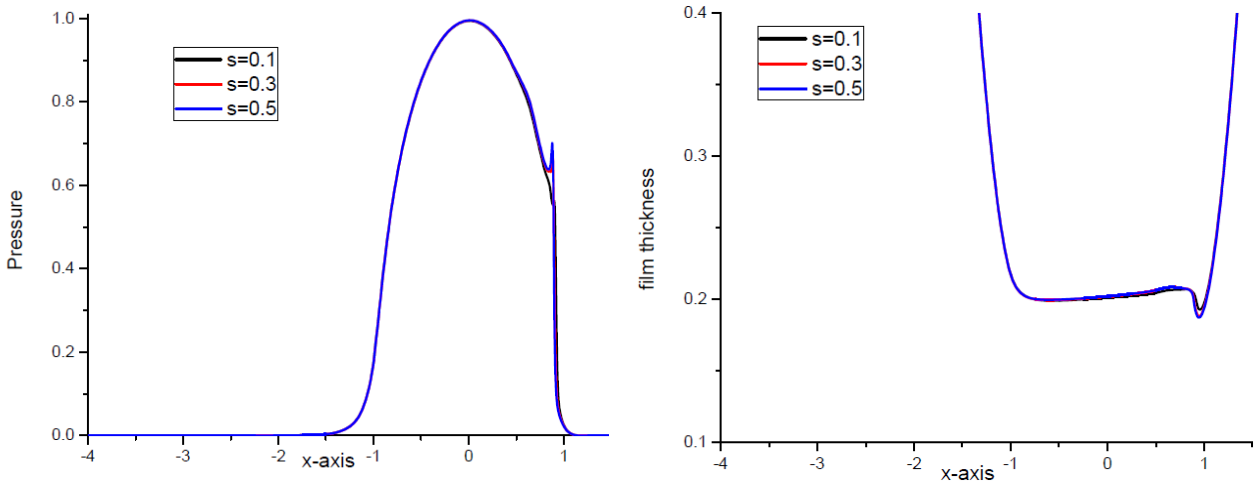

Figure 7(a, b). Thermal pressure and film thickness profile for varying s at U=2E-11,W=2E-04, Lm=1E-4.

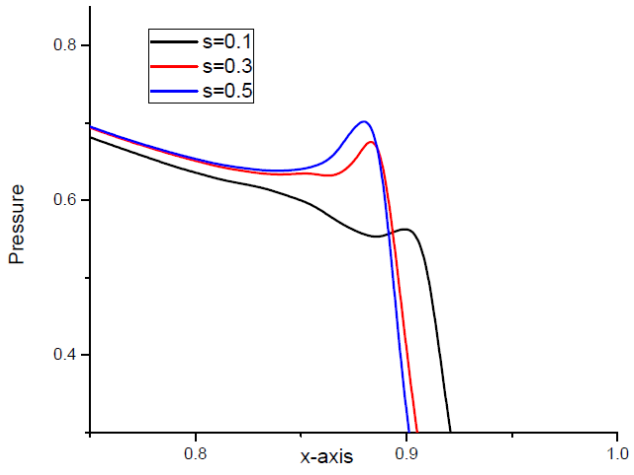

Figure 8. Thermal pressure spike profile for varying s, at U=2E-11, W=2E-04 and *Lm*=1E-04.

6. Conclusions

FAS is one of the most efficient algorithms of low complexity for the analysis of more involved EHL problems, which overcomes the limitation of conventional numerical schemes. The observations such as a decrease in height and spread of pressure spike and shift of its location (or maximum value) towards the center of the contact region for an increase in s, the slide-roll ratio (or moving bearing surfaces), is a useful prediction in design of bearings. Pressure spike increases with increase s, the slide-roll ratio. The rise in temperature decreases with increasing s with couple stress fluid as a lubricant (compared with viscous cases), whereas the pressure spike shifts towards exit for the increase in load and speed and is almost dimensionless in height as well as in spread. Minimum film thickness decreases with thermal effects but with non-Newtonian aspect of the lubricant, minimum film thickness increases with an increase in L_m the couple stress parameter. These predictors can serve as a sort of input information for the bearing designers.

Nomenclature

b half width of the Hertzian contact zone, $b=\left[8wR/(\pi E')\right]^{1/2}$

E' effective elastic modulus of roller and disc, $\frac{1}{E'}=\frac{1}{2}\left(\frac{1-v_1^2}{E_1}+\frac{1-v_2^2}{E_2}\right)$

$E_{1,2}$ elastic modulus of solids

h film thickness

H dimensionless film thickness

L_m couple stress parameter

G material parameter, $G=\alpha E'$

P dimensionless pressure, $\frac{p}{p_H}$

p pressure

p_H maximumHertzian pressure, $p_H=2w/\pi b$

R reduced radius of curvature in the x-direction

t temperature

T_0 inlet temperature of the lubricant

T dimensionless temperature, $T=\frac{t}{T_0}$

U dimensionless speed parameter $U=\eta_0 u_m/(E'R)$

u_m average entrainment speed $u_m=(u_a+u_b)/2$

$u_{a,b}$ lower and upper surface speed.

s sliding/rolling ratio

w applied load per unit length

W dimensionless load parameter $W=w/(E'R)$

α pressure viscosity parameter

X dimensionless-ordinate, $X=\frac{x}{b}$

ΔX space increment

$\overline{Z}$ dimensionless coordinate, $\overline{Z}=\frac{z}{H}$,

$\Delta\overline{Z}$ increment along z axis

Greek symbols

α pressure viscosity index

β thermal—density coefficient

γ thermal-viscosity coefficient of lubricant

$k_{1,2}$ thermal conductivity of rollers

k_f thermal conductivity of lubricant

$\rho_{a,b}$ density of solids

$\upsilon_{1,2}$ Poisson's ratio of solids

τ shear stress

$c_{1,2}$ specific heat of solids

η viscosity of lubricant

η_0 viscosity at ambient pressure

$\overline{\eta}$ dimensionless viscosity

ρ density of lubricant

ρ_0 inlet density of pressure

$\overline{\rho}$ dimensionless density

c_p specific heat of lubricant

λ_a molecular length of additive.

$\overline{\tau}$ $=\frac{\tau}{E'}$

Conflict of Interest

There is no conflict of interest.

References

[1] Dowson, D., Higginson, G.R., 1997. Elastohydrodynamic lubrication, second edition. Pergamon Press: Oxford.

[2] Hamrock, B.J., Tripp, J.H., 1983. Numerical methods and computers used in Elastohydrodynamic lubrication. Proceedings 10th leeds Lyon Symposium, Tribology. Butterworth Scientific Ltd.: London. pp. 11-19.

[3] Dowson, D., Ehrel, P., 1999. Present and future studies in Elastohydrodynamic lubrication. Proceedings of the Institution of Mechanical Engineers Part J-Journal of Engineering Tribology. 213, 317-333.

[4] Schlijper, A.G., Series, L.E., Rycrist, J.E., 1996. Current tools and techniques in EHL modeling. Tribology International. 29(8), 669-673.

[5] Spikes, H.A., 2006. Sixty years of EHL. Lubrication Science. 18, 265-291.

[6] Lugt, P.M., Morales-Espejel, G.E., 2011. A review of Elastohydrodynamic theory. Tribology Transaction. 54, 478-496.

[7] Venner, C.H., 1991. Multilevel solution of the EHL line and point contact problems [PhD thesis]. Netherland: Twente University.

[8] Goodyer, C.E., 2001. Adaptive numerical methods for EHL [PhD thesis]. Leeds: University of Leeds.

[9] Petrusevich, A.I., 1951. Fundamental conclusions from the contact hydrodynamic theory of lubrication. IZV.Akad. Mank, SSSR (Ctal). 2, 209-223.

[10] Okamura, H.A., 1982. Contribution to the numerical analysis of isothermal elastohydrodynamic lubrication. Tribology of reciprocating rngines. Proceedings of the 9th Leeds-Lyon Symposium on Tribology. Butterworth Scientific Ltd.: London. pp. 313-320.

[11] Lubrecht, A.A., Ten Napel, W.E., Bosma, R., 1986. Multigrid, an alternating method for calculating film thickness and pressure profiles in elastodyrodynamically lubricated line contacts. Journal of Tribolgy. 108, 551-556.

[12] Brandt, A., 1984. Multigrid Techniques: 1984, Guide with application to fluid dynamics. GMD Bonn.

[13] Brandt, A., Lubrecht, A.A., 1990. Multilevel matrix multiplication and fast solution of integral equations. Journal of Computational Physics. 90, 348-370.

[14] Venner, C.H., Ten Napel, W.E., Bosma, R., 1990. Advanced multilevel solution of the EHL line contact problem. Transaction of the ASME. 112, 426-432.

[15] Bujurk, N.M., Shettar, B.M., Kantli, M.H., 2017. Wavelet preconditioned Newton-Krylov method for EHL line contact problems. Applied Mathematical Modeling. 46, 285-298.

[16] Bell, J.C., 1962. Lubrication of rolling surfaces by a Ree-Eyring fluid. ASLE Transactions. 5, 160-171.

[17] Houpert, L.G., Hamrock, B.J., 1985. Elastohydrodynamic lubrication calculation used as a tool to study scffing. Proceedings 12th Leeds Lyon symposium on Tribology. Butterworth Scientific Ltd.: London. pp. 146-159.

[18] Conry, T.F., Wang, S., Cusano, C., 1987. A Reynolds-Eyring equation for elastohydrodynamic lubrication in line contacts. Transaction ASME, Journal of Tribology. 109, 648-658.

[19] Jacobson, B.O., Hamrock, B.J., 1984. Non-Newtonian fluid model incorporated into elastohydrodynamic lubrication of rectangular contacts. ASME Journal of Tribology. 106(2), 275-284.

[20] Zhu, W.S., Neng, Y.T., 1988. A Theoretical and experimental study of EHL with grease. Transaction ASME Journal of Tribology. 110, 38-43.

[21] Bujurke, N.M., Shettar, B.M., Hiremath, P.S., 2018. A novel numerical scheme for the analysis of effects of surface roughness on EHL line contact with couple stress fluid as lubricant. Indian Academy of Sciences, Saadhana. 43, 1-22. doi: 10.1007/s12046-018-0906.

[22] Wang, S.H., Hua, D.Y., Zhang, H.H., 1988. A

full numerical EHL solution for the line contacts under pure rolling condition with a Non-Newtonian Rheological Model. Journal of Tribology. 110(4), 583-586.

[23] Chippa, S.P., Sarangi. M., 2013. Elastohydrodynamically lubricated finite line contact with couple stress fluids. Tribology International. 67, 11-20.

[24] Das, N.C., 1997. Elastohydrodynamic lubrication theory of line contacts couple stress fluid model. Tribology Transaction. 40, 353-359.

[25] Saini, P.K., Kumar, P., Tandon, P., 2007. Thermal elastohydrodynamic lubrication characteristics of couple stress fluid in rolling/sliding line contacts. Proceedings of the Institution of Mechanical Engineers—Part J, Journal of Engineering Tribology. 221, 141-153.

[26] Kantli, M.H., Shettar, B.M., Bujurke, N.M., 2017. Jacobian free Newton-GMRES method for analyzing combined effects of surface roughness and couple stress character of lubricant on EHL line contact. INSA. 83, 175-196.

[27] Bujurke, N.M., Kantli, M.H., Shettar, B.M., 2018. Jacobian free Newton-GMRES method for the solution of elastohydrodynamic grease lubrication in line contact using wavelet based preconditioner. Proc. Acad. Sci. A Phy. Sci. 88(2), 247-265.

[28] Awati, V.B., Shankar, N., Mahesh Kumar, N., 2016. Multigrid method for the EHL line contact with bio-based oil as lubricant. Applied Mathematics and Nonlinear Science. 1(2), 359-368.

[29] Awati, V.B., Shankar, N., Mahesh Kumar, N., 2018. Multigrid method for the solution of EHL point contact with bio-based oil as lubricants for smooth and rough asperity. Industrial Lubrication and Tribology. 70(4), 599-611. doi: 10.1108/ILT-12-2016-0314.

[30] Awati, V.B., Shankar, N., 2018. An Isothermal Elastohydrodynamic lubrication of elliptical contact with multigrid method. Australian Journal of Mechanical Engineering. 18(3), 375-384. doi: 10.1080/14484846.2018.1531810.

[31] Sternlicht, B., Lewis, P., Flynn, P., 1961. Theory of lubrication and failure of rolling contacts. ASME Transaction of Tribology. 83, 213-226.

[32] Cheng, H.S., Sternlicht, B., 1965. A numerical solution for the pressure, temperature and film thickness between two infinitely long, lubricated rolling and sliding cylinders, under heavy loads. Journal of Basic Engineering. 87, 695-707.

[33] Dowson, D., Whitaker, A.V., 1968. A numerical procedure for the solution of the elastohydrodynamic problem of rolling and sliding contact lubricated by a Newtonian fluid. Proceedings of the Institution of Mechanical Engineers. 182, 119-134.

[34] Murch, L.E., Wilson, W.R.D., 1975. A thermal elastohydrodynamic inlet zone analysis. ASME Journal of Lubrication Technology. 97, 212-216.

[35] Ghosh, M.K., Hamrock, B.J., 1985. Thermal elastohydrodynamic lubrication of line contacts. ASLE Transaction. 28, 159-171.

[36] Sadeghi, F., Sui, P.C., 1990. Thermal elastohydrodynamic lubrication of rolling/sliding contacts. ASME Journal of Tribology. 112, 189-195.

[37] Houpert, L.G., Hamrock, B.J., 1986. Fast approach for calculating film thickness and pressures in elastohydrodynamically lubricated contacts at high load. Journal of Tribology. 108, 411-420.

[38] Yang, P.R., Wen, S.H., 1992. The behavior of non-Newtonian thermal EHL film in line contacts as dynamic loads. ASME, Journal of Tribology. 114, 81-85.

[39] Wolff, R., Nonaka, T., Kubo, A., et al., 1992. Thermal elastohydrodynamic lubrication of rolling/sliding line contacts. ASME Journal of Tribology. 114, 706-713.

[40] Wolff, R., Kubo, A., 1994. The application of Newton-Raphson method to thermal elastohydrodynamic lubrication of line contacts. ASME Journal of Tribology. 116, 733-740.

[41] Hsiao, H.S., Hamrock, B.J., 1994. Non-Newtonian and thermal effects on film generation and traction reduction in EHL line contacts conjunction. ASME Journal of Tribology. 116(4), 794-823.

[42] Yang, P., Wang, T., Kaneta, M., 1994. Thermal and non-Newtonian numerical analysis for starred EHL line contact. ASME Journal of Tribology. 128(2), 282-298.

[43] Salehizadeh, H., Saka, N., 1991. Thermal non-Newtonian elastohydrodynamic lubrication of rolling line contacts. ASME, Journal of Tribology. 113, 481-491.

[44] Liu, Z., Picken, D., He, T., et al., 2018. A thermal EHL model for connected rollers and its application on open seal-Houling interface. Journal of Tribology. 30, 1-34.

[45] Briggs, W.L., Henson, V.E., McCormick, S.F., 2000. A multigrid tutorial, second edition. SIAM: Philadelphia.

[46] Roelands, C.J.A., 1966. Correlation aspects of viscosity-temperature-pressure relationship of lubricating oils [PhD thesis]. Netherlands: Delft University of Technology.

[47] Wang, S.H., Zhang, H.H., 1987. Combined effects of thermal and non-Newtonian character of lubricant on pressure, film profile, temperature rise and shear stress in EHL. Journal of Tribology. 109, 666-670.

[48] Carslaw, H., Jaeger, J.C., 1959. Conduction of heat in solids. Oxford University Press: Oxford.

[49] Bisset, E.J., Glander, D.W., 1998. A highly accurate approach that resolves the u6pressure spike of EHL. Transaction, ASME, Journal of Tribolog. 110, 241-246.

[50] Venner, C.H., Ten Napel, W.E., 1989. Numerical calculation of the pressure spike in EHL. Lubrication Science. 2, 321-334.